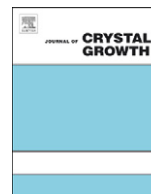




ELSEVIER

Contents lists available at ScienceDirect

## Journal of Crystal Growth

journal homepage: [www.elsevier.com/locate/jcrysgro](http://www.elsevier.com/locate/jcrysgro)

# Improvement of *a*-plane GaN crystalline quality by overgrowth of *in situ* etched GaN template

Hsiao-Chiu Hsu<sup>a</sup>, Yan-Kuin Su<sup>a,b,\*</sup>, Shyh-Jer Huang<sup>a</sup>, Shin-Hao Cheng<sup>b</sup>, Chiao-Yang Cheng<sup>a</sup>

<sup>a</sup> Institute of Microelectronics, Department of Electrical Engineering, and Advanced Optoelectronic Technology Center, National Cheng Kung University, Tainan 701, Taiwan

<sup>b</sup> Department of Electrical Engineering, Kun Shan University of Technology, Yung-Kang, Tainan 710, Taiwan

## ARTICLE INFO

Available online 17 September 2010

## Keywords:

- A1. Etching
- A3. Metalorganic vapor phase epitaxy
- B1. Nitrides
- B2. Semiconducting III–V materials

## ABSTRACT

This study demonstrates improvement of crystalline quality of *a*-plane GaN by growing it on a porous GaN template fabricated by *in situ* etching of a first GaN film using hydrogen and ammonia gases at 1150 °C in a metal organic chemical vapor deposition (MOCVD) reactor. Photoluminescence (PL) and high-resolution X-ray diffraction (HR-XRD) measurements show that the crystalline quality of the GaN film re-grown on the porous GaN template was superior to the quality of the initially grown GaN film. This study demonstrates a simple, short procedure for growing high quality *a*-GaN using a single MOCVD tool without *ex situ* processes.

© 2010 Elsevier B.V. All rights reserved.

## 1. Introduction

Group-III-nitride based materials have been widely used in optoelectronic devices in recent years [1]. Wurtzite structured nitride material has strong piezoelectric properties and experiences spontaneous polarization along the *c*-axis, resulting in a large quantum-confined Stark effect [2]. In non-polar (*a*-axis or *m*-axis) nitrides, the *c*-axis lies parallel to the quantum well, leading to an absence of polarization, a phenomenon that is of considerable interest to researchers [3]. However, non-polar GaN contains very high density of threading dislocations (TD) (in the range of  $10^9$ – $10^{10}$  cm<sup>-2</sup>) and stacking faults (SF) ( $10^5$  cm<sup>-1</sup>), due to the planar anisotropic nature of its growth and differing lattice and thermal expansion coefficients between the GaN film and sapphire substrate. Therefore, researchers have devised diverse methods to overcome this problem, such as selection of suitable buffer layers [4,5] or various patterns leading to lateral growth, which have provided improvements in crystal quality. Epitaxial lateral overgrowth (ELOG) [6,7] and other modified ELOG techniques such as sidewall ELOG [8], one-sidewall-seed ELOG [9] and nanorod ELOG [10] have been developed to minimize dislocation density (DD). While these ELOG techniques can improve surface morphology and reduce dislocation densities, the approach is excessively complicated and time-consuming.

Recently, research groups have demonstrated that crystalline quality of a GaN epitaxial film re-grown on porous substrate [11], or defect-related pits [12] could be improved by lateral overgrowth

or selective growth. In this report, we demonstrate improvements in *a*-plane GaN crystalline quality using MOCVD on *in situ* etched porous GaN template. The MOCVD-GaN template is etched *in situ* at high temperature with a H<sub>2</sub>/NH<sub>3</sub> gas mixture to fabricate a porous GaN template. Size and density of the etched pits were investigated with varying H<sub>2</sub>/NH<sub>3</sub> ratio. Compared to previously reported methods, this method is a highly efficient process, as the *a*-plane GaN film can be etched and re-grown in a single chamber without additional processing.

## 2. Experimental procedure

All *a*-plane GaN films were grown on *r*-plane sapphire (within  $\pm 0.5^\circ$ ) using an MOCVD reactor. Trimethylgallium (TMGa) and ammonia (NH<sub>3</sub>) acted as precursors with hydrogen (H<sub>2</sub>) as the carrier gas during the entire epitaxial process. The thickness of the initially grown GaN was 1.4 μm and its epitaxial growth conditions were detailed in a previous paper [13]. To fabricate the porous GaN template, a H<sub>2</sub>/NH<sub>3</sub> etching gas mixture was injected at a fixed temperature of 1150 °C for 30 min. The upper *a*-plane GaN film was grown on the *in-situ*-etched template by injecting TMGa/NH<sub>3</sub> gas into the reactor at 1150 °C for 1 h. The V/III ratio of re-grown GaN was kept low to enhance the lateral overgrowth mode during the epitaxial process. For comparison, an *a*-plane GaN film of the same thickness was also grown covering the non-*in-situ*-etched initial 1.4 μm GaN, labeled as the single-growth GaN. Scanning electron microscopy (SEM) was used to observe the surface morphology and film structure of these samples. Crystalline qualities of single-growth and re-grown GaN were then compared by PL and HR-XRD at room temperature.

\* Corresponding author.

E-mail address: [yksu@mail.ncku.edu.tw](mailto:yksu@mail.ncku.edu.tw) (Y.-K. Su).

Distributions of defects in single-growth and re-grown GaN were observed by transmission electron microscopy (TEM).

### 3. Results and discussion

Fig. 1 shows the plan-view SEM images of initially grown *a*-plane GaN films before and after *in situ* thermal etching. Prior to etching, the initially grown *a*-plane GaN film surface was smooth and pit-free, as shown in Fig. 1(a). To fabricate a porous GaN template, an *a*-plane GaN film was etched using pure H<sub>2</sub> at 1150 °C for 30 min, Fig. 1(b). Analysis of the plan-view SEM image and energy dispersive spectrometry (EDS) revealed that gallium metal droplets were present on the film surface. The diameter of the droplets was approximately 3–5 μm. This occurred because GaN can decompose to Ga (vapor phase) and NH<sub>3</sub> (vapor phase) when reacting with hydrogen gas at elevated temperatures, which leads to etching of the GaN film [14]. To control the etching process, the gas should be modified from pure H<sub>2</sub> gas to an H<sub>2</sub>/NH<sub>3</sub> gas mixture. Due to differing bonding energies (Ga–N) at different surface sites, adding NH<sub>3</sub> gas to control the etching process may result in selective etching in defect-rich regions compared to defect-free regions. If this happens, the initial porous GaN template will play an important role in reducing the dislocation density in the re-grown *a*-plane GaN film. Weyher et al. [12] studied the influence of cross-sectional shape on the re-grown GaN film, and reported that, compared to overgrowth

on shallower and narrower etch pits, overgrowth on the template with deeper and larger etch pits could avoid the dislocations in the initially-grown film threading into the new GaN layer. In their study, dislocations could be interrupted by voids resulting from incomplete filling of the etched pits during the re-growth process. Hence, a higher pit density could interrupt a greater number of dislocations. To investigate the effect of reactor conditions on etch pit density and shape of etched pits, the etched time was fixed at 30 min, while the composition ratio of the etching gas was varied. Figs. 1(c), (d) and (e) show the surface morphology of etched GaN templates with H<sub>2</sub>/NH<sub>3</sub> ratios of 100/1, 50/1 and 10/1, respectively. The morphology of *a*-plane GaN film following *in situ* thermal etching is distinct from that of *c*-plane GaN after a similar etching process, which presents many pyramidal protrusions on the surface [15]. Fig. 1(d) shows some inverse-pyramidal pits and

**Table 1**

Characteristics of etched porous template treated with different etch procedures.

| Etch procedure | H <sub>2</sub> /NH <sub>3</sub> | Time (min) | Pit density (cm <sup>-2</sup> ) | Pit size along [1̄100] (μm) |
|----------------|---------------------------------|------------|---------------------------------|-----------------------------|
| A              | 100/1                           | 30         | $5.4 \times 10^5$               | 3–5                         |
| B              | 50/1                            | 30         | $5.6 \times 10^6$               | 0.8–1.2                     |
| C              | 10/1                            | 30         | $2.2 \times 10^7$               | 0.1–0.3                     |
| D              | 50/1                            | 20         | $7.2 \times 10^6$               | 1.4–3.2                     |
|                | 100/1                           | 10         |                                 |                             |

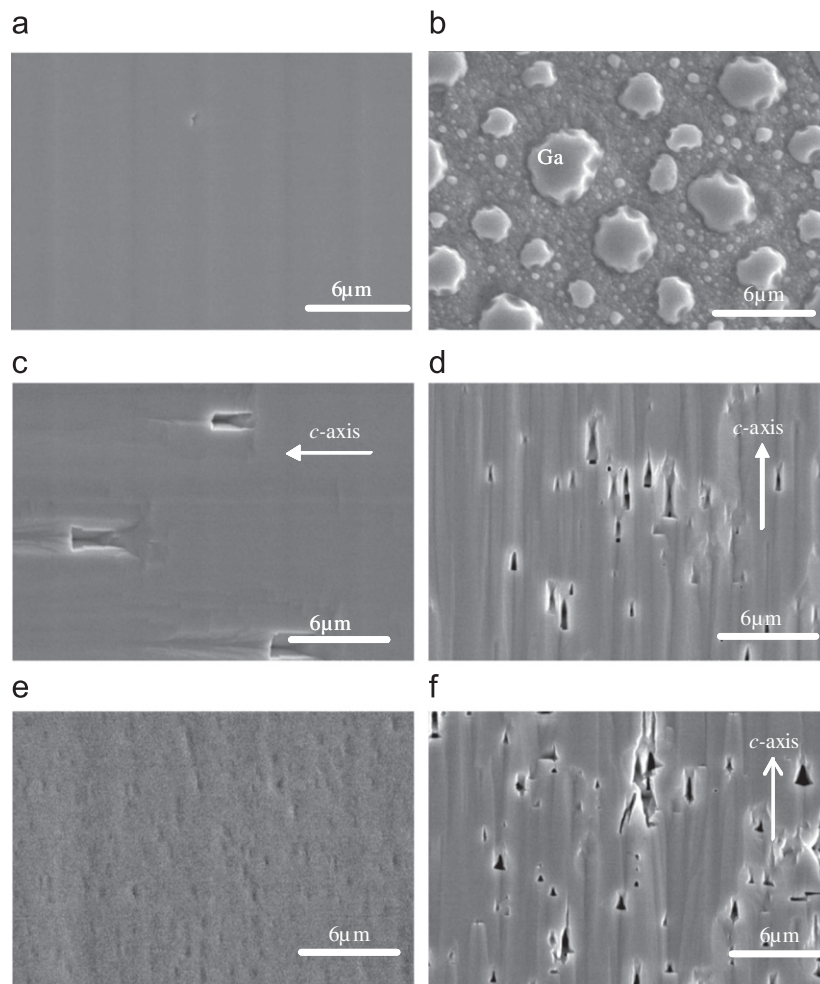


**Fig. 1.** Plan-view SEM images of (a) initially grown GaN template, the porous GaN templates etched for 30 min under pure H<sub>2</sub> gas and H<sub>2</sub>/NH<sub>3</sub> mixture with ratios in one step of (b) 100/1, (c) 50/1, (d) 10/1, and (e) etched with H<sub>2</sub>/NH<sub>3</sub> mixture gas in two steps.

stripe-like patterns along the *c*-axis that appeared on the surface. The size and density of the etched pits, for varying gas ratios, are listed in Table 1 (etch procedures A–C). The size of etched pits decreased with a decrease in  $H_2/NH_3$  ratio. By contrast, the etch pit density increased as the  $H_2/NH_3$  ratio decreased. Compared

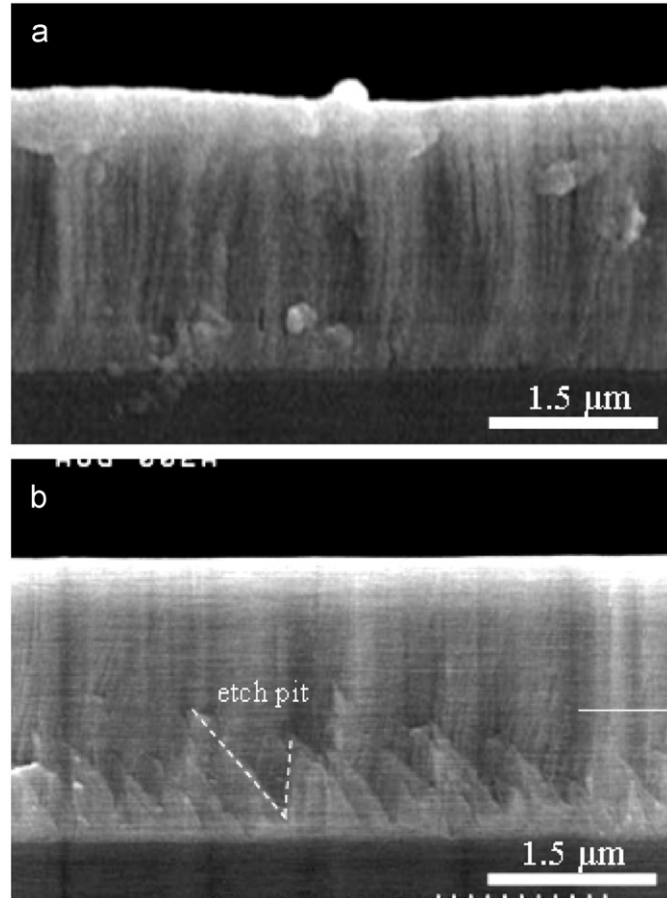


Fig. 2. Cross-sectional SEM images of (a) single-growth GaN and (b) re-grown GaN samples.

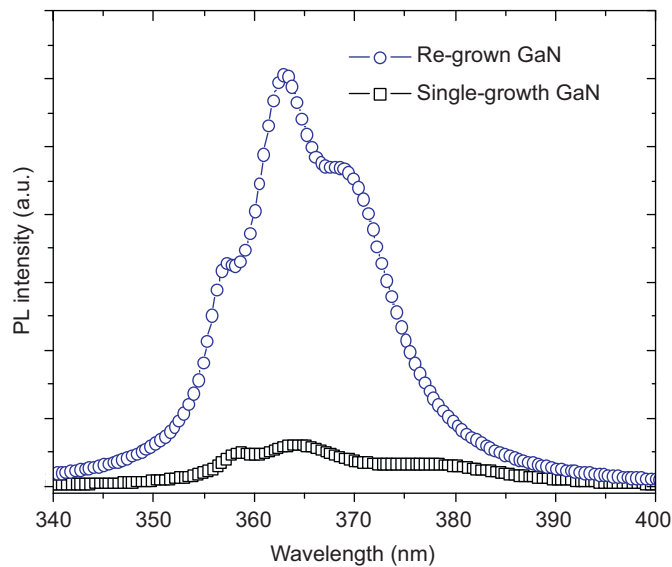


Fig. 3. Room temperature PL spectra of single-growth GaN and re-grown GaN samples.

with other gas mixture ratios, the etched pits with the mixture  $H_2/NH_3$  ratio of 100/1 were deeper and larger, but their density was the lowest. In order to enhance both density and size of etch pits on porous GaN template, the one-step etch procedure was modified to a two-step procedure (etch procedure D, Table 1). Fig. 1(f) shows a plan-view SEM image of the porous GaN template after two-step etching. The etch pit density was  $7.2 \times 10^6 \text{ cm}^{-2}$  and the etch pit sizes were between 1.4 and 3.2  $\mu\text{m}$ , as detailed in Table 1. The depth of etch pits was  $> 1 \mu\text{m}$  by cross-sectional SEM image (not shown here).

Fig. 2 shows cross-sectional SEM images of single-growth and re-grown GaN films. Film thicknesses of these two samples were comparable, at approximately 2.48  $\mu\text{m}$ . The cross-section of the GaN film re-grown from the etched porous GaN template using lateral growth mode is shown in Fig. 2(b). The interface between the re-grown film and porous GaN template is clearly observable after re-growth. Additionally, it was apparent that fabrication of a GaN template with deep, large etch pits was successful, as indicated by the dashed line in Fig. 2(b).

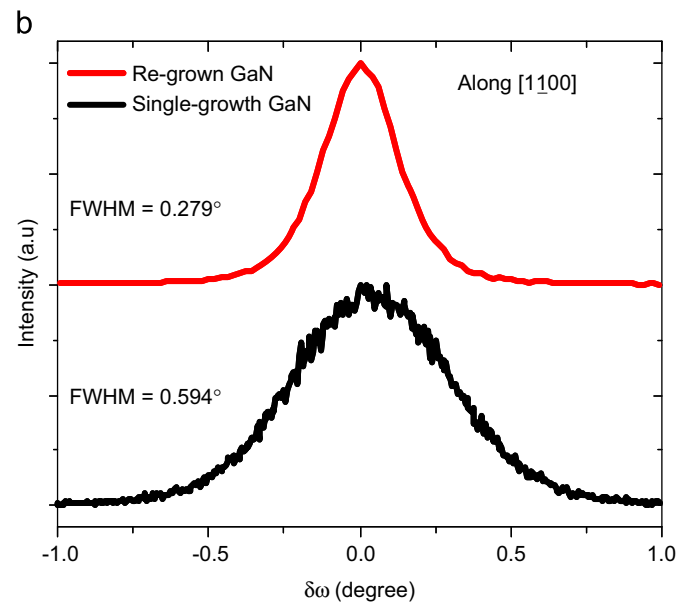
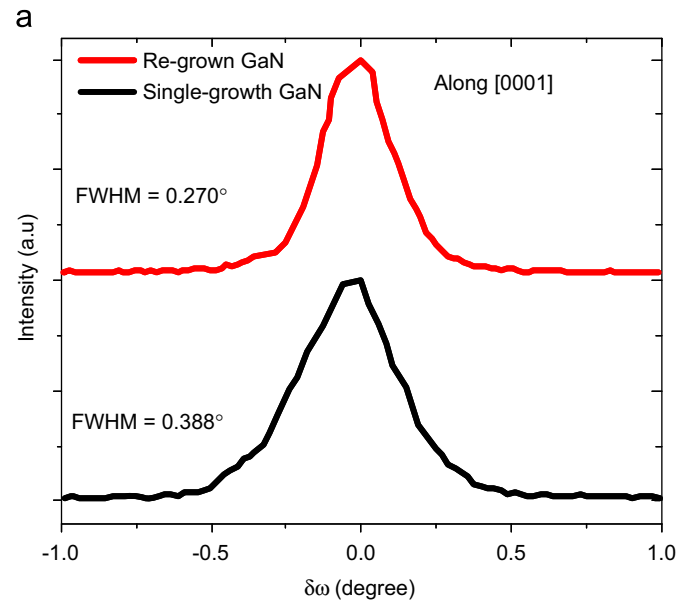
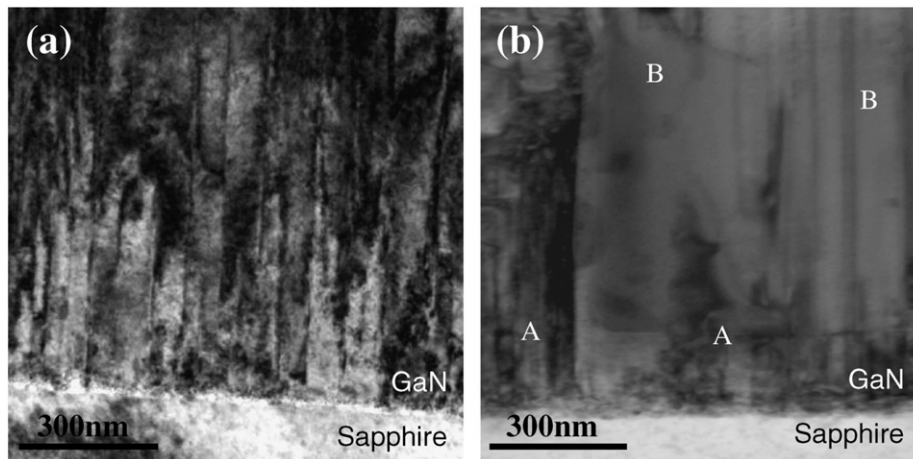


Fig. 4. Omega curves of single-growth and re-grown samples along (a) *c*-axis and (b) *m*-axis.



**Fig. 5.** Cross-sectional TEM images of (a) single-growth GaN and (b) re-grown GaN sample. Re-grown GaN film has been divided into initially grown region (A) and re-grown region (B).

Fig. 3 shows the room-temperature PL spectra of the single-growth and the re-grown *a*-plane GaN films. The PL spectra show that the intensity of the main emission from the re-grown film was six times greater than that of the single-growth film. The sample re-grown on the etched porous GaN template exhibited strong band-edge emission, due to improved crystal quality. The enhancement of emission intensity could be due to improved crystalline quality, with fewer TDs, which play a role as non-radiative centers.

To analyze crystal quality, FWHMs of omega ( $\omega$ ) scans along *c*-axis ([0 0 0 1])/*m*-axis ([1  $\bar{1}$  0 0]) were measured by HR-XRD, as shown in Fig. 4. The FWHMs were reduced from  $0.388^\circ$  (*c*-axis) and  $0.594^\circ$  (*m*-axis) for the single-growth sample to  $0.270^\circ$  and  $0.279^\circ$  in the re-grown sample, respectively. A greater reduction of FWHM occurred along the *m*-axis than the *c*-axis. This might be due to the ease of coalescence of the re-grown GaN films along the *m*-axis, since width of the etched pits along the *m*-axis is narrower than it is along the *c*-axis.

Fig. 5 shows in a cross-sectional TEM image the distribution of defects of the single-growth and re-grown GaN film. Fig. 5(a) shows single-growth film dislocations propagating from the substrate and travelling upward. However, the TEM image of the re-grown film is different from the image of the single-growth film, as shown in Fig. 5(b). The TEM image could be divided into two regions: the initially grown region (A) and the re-grown region (B). Some boundaries between dislocations and the re-grown film caused by the overlying GaN coalesced over the fringe of the porous GaN template with deep etch pits. The average density of dislocations of the re-grown film was 1–2 orders of magnitude lower than in the single-growth film. Overall quantity of dislocations in the re-grown film was less than in the single-growth film, indicating that crystal quality had improved through lateral overgrowth on the porous template.

#### 4. Conclusions

This study demonstrated a simple method to improve crystalline quality of *a*-plane GaN film by re-growth on a GaN template etched *in situ* in an MOCVD reactor. The etched porous GaN template was fabricated with an  $\text{H}_2/\text{NH}_3$  etching gas mixture at  $1150^\circ\text{C}$ . The size and density of etch pits varied with the  $\text{H}_2/\text{NH}_3$  ratio. Omega FWHM values along the *c*- and *m*-axes of the

re-grown GaN film were both reduced. TEM images demonstrated that density of defects on the re-grown film had been reduced by overgrowth on the etched porous GaN film. The re-grown *a*-plane GaN film on *in situ* etched porous GaN template showed enhanced luminescent intensity and strong band-edge emission as well as an improvement in crystalline quality. All the above results demonstrate that the overgrowth method on *in situ* etched porous GaN template could serve as a simple, accelerated process for the improvement of *a*-plane GaN crystalline quality.

#### Acknowledgments

The authors would like to thank the National Science Council, Bureau of Energy, Ministry of Economic Affairs, Taiwan, for financial support under Contract no. 98-D0204-6 and TDPA Program nos. 97-EC-17-A-07-S1-105 and NSC 97-2623-E-168-001-IT. The assistance in devices characterization provided by the LED Lighting and Research Center, NCKU is also appreciated.

#### References

- [1] S.F. Chichibu, T. Sota, K. Wada, O. Brandt, K.H. Ploog, S.P. DenBaars, S. Nakamura, *Phys. Status Solidi A* 183 (2001) 91.
- [2] F. Bernardini, V. Fiorentini, D. Vanderbilt, *Phys. Rev. B* 56 (1997) R10024.
- [3] A. Chakraborty, B.A. Haskell, S. Keller, J.S. Speck, S.P. DenBaars, S. Nakamura, U.K. Mishra, *Appl. Phys. Lett.* 85 (2004) 5143.
- [4] X. Ni, Y. Fu, Y.T. Moon, N. Biyikli, H. Morko, *J. Cryst. Growth* 290 (2006) 166.
- [5] F. Wu, M.D. Craven, S.H. Lim, J.S. Speck, *J. Appl. Phys.* 94 (2003) 942.
- [6] X. Ni, U. Ozgur, Y. Fu, N. Biyikli, J. Xie, A.A. Baski, H. Morkoc, Z. Liliental-Weber, *Appl. Phys. Lett.* 89 (2006) 262105.
- [7] T. Wernicke, U. Zeimer, C. Netzel, F. Brunner, A. Knauer, M. Weyers, M. Kneissl, *J. Cryst. Growth* 311 (2009) 2895.
- [8] D. Iida, A. Miura, Y. Okadome, Y. Tsuchiya, T. Kawashima, T. Nagai, M. Iwaya, S. Kamiyama, H. Amano, I. Akasaki, *Phys. Status Solidi A* 204 (2007) 2005.
- [9] D. Iida, M. Iwaya, S. Kamiyama, H. Amano, I. Akasaki, *J. Cryst. Growth* 311 (2009) 2887.
- [10] S.C. Ling, C.L. Chao, J.R. Chen, P.C. Liu, T.S. Ko, T.C. Lu, H.C. Kuo, S.C. Wang, S.J. Cheng, J.D. Tsay, *Appl. Phys. Lett.* 94 (2009) 251912.
- [11] Y.D. Wang, K.Y. Zang, S.J. Chua, S. Tripathy, P. Chen, C.G. Fonstad, *Appl. Phys. Lett.* 87 (2005) 251915.
- [12] J.L. Weyher, H. Ashraf, P.R. Hageman, *Appl. Phys. Lett.* 95 (2009) 031913.
- [13] H.C. Hsu, Y.K. Su, S.J. Huang, Y.J. Wang, C.Y. Wu, M.C. Chou, *Jpn. J. Appl. Phys.* 49 (2010) 04DH05.
- [14] C.D. Thurmond, R.A. Logan, *J. Electrochem. Soc.* 119 (1972) 622.
- [15] Y.T. Moon, Y. Fu, F. Yun, S. Dogan, M. Mikkelsen, D. Johnstone, H. Morko, *Phys. Status Solidi A* 202 (2005) 718.